Inorganic Chemistry

Communication

Cite This: Inorg. Chem. XXXX, XXX, XXX−XXX

pubs.acs.org/IC

Chiral Metal−Organic Framework Decorated with TEMPO Radicals for Sequential Oxidation/Asymmetric Cyanation Catalysis

Zijian Li,[†] Yan Liu,*[,†] Xing Kang,[†] and Yong Cui*[,†,‡]

[†]School of Chemistry and Chemical Engineering and State Key Laboratory of Metal Matrix Composites, Shanghai Jiao Tong University, Shanghai 200240, China

[‡]Collaborative Innovation Center of Chemical Science and Engineering, Tianjin 300072, China

Supporting Information

ABSTRACT: A chiral porous metal−organic framework (MOF) decorated with radicals has been successfully constructed by cocrystallizing achiral (2,2,6,6-tetramethylpiperidin-1-yl)oxyl (TEMPO)-substituted tricarboxylate and enantiopure VO(salen)-derived dipyridine ligands. The chiral MOF can function as an efficient heterogeneous catalyst for the sequential alcohol oxidation/asymmetric cyanation of aldehyde reactions with enhanced activity and enantioselectivity compared to the homogeneous counterpart.

Crystalline metal−organic frameworks (MOFs) have been actively studied in recent decades because of their modular nature, facile tunability, and diverse applications.[1] One of the current trends in MOF-based catalysis is to emulate nature by developing multicatalysis systems, wherein multiactive sites are combined into a single network, for sequential/tandem transformations.[2] The precise incorporation of multiple active sites at the metal nodes and/or organic linkers can provide an additional synergistic cooperation effect, thus achieving improved activities and stereoselectivities over monocatalytic systems, especially for asymmetric catalysis.[2,3] However, examples of chiral multifunctional MOF catalysts are still rather rare, mainly because of the difficulty in controlling the proper proximity and conformation of active sites to create effective cooperative activation.[3]

Given the widespread importance of stable organic radicals in optics, electronics, magnetics, and catalysis, the exploration of radical-immobilized solid materials with extraordinary and fascinating properties is highly desirable.[4,5] Although considerable efforts devoted to this area over the past years have led to some potentially useful radical materials, only a few examples of MOFs with radicals as the building units have been reported to date.[5] Some typical examples for catalysis applications have recently been presented by Kitagawa and Chmielewski, in which nitroxide-radical-decorated/appended MOFs were successfully fabricated for the aerobic oxidation of alcohols.[5c,d] In this work, a chiral MOF featuring both stable organic radicals and chiral metallosalen catalysts was synthesized for the first time, which can be applied to prompt sequential alcohol oxidation/asymmetric cyanation of aldehyde reactions with excellent catalytic efficiency and high enantioselectivity.

Scheme 1. Structures of the Organic Linkers H_3L^1 and VOL^2

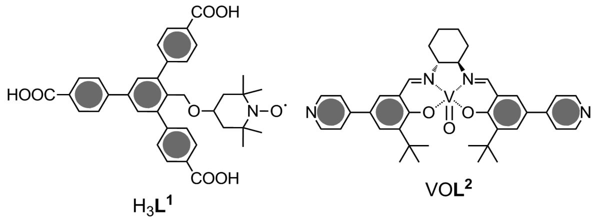

Heating a mixture of H_3L^1, VOL^2 (Scheme 1), and $Cd(NO_3)_2 \cdot 6H_2O$ in dimethylacetamide (DMA)/methanol (MeOH) at 80 °C afforded olive-green crystals of $[Cd_4(L^1)_2(VOL^2)_4(NO_3)_2(DMA)_2]\cdot(DMA)_2\cdot(MeOH)_2\cdot(H_2O)_5$ (**1**). The product is stable in air as well as in various common solvents including water. The formulation of **1** was confirmed by elemental analysis, thermogravimetric analysis (TGA), and IR spectroscopy, and powder X-ray diffraction (PXRD) analysis indicated the pure phase of its bulk sample.

Single-crystal X-ray analysis on **1** reveals that it crystallizes in the monoclinic chiral space group C2. The four crystallographically independent Cd atoms all adopt a distorted pentagonal-bipyramid geometry coordinated by two axial N atoms of two VOL^2 ligands and five equatorial O atoms from three L^1 ligands for Cd1 and Cd2 or five O atoms from one L^1 ligand, one DMA, and one NO_3^- anion for Cd3 and Cd4. Cd1 and Cd2 are bridged by a pair of μ_2-η^1,η^2-carboxylate groups of two L^1 ligands into a binuclear $\{Cd_2\}$ subunit, and neighboring $\{Cd_2\}$ units are doubly interlinked by L^1 ligands to form an infinite ribbonlike chain (Figure 1a). The L^1 ligand in **1** exhibits only one bridging mode (one tridentate and two chelating bidentate carboxylate groups), binding to two $\{Cd_2\}$ units in one ribbon and one Cd3 or Cd4 node via its three carboxylate groups, respectively. Adjacent ribbons are further linked by the coordination of VOL^2 ligands, in which each V center lies in a square-pyramidal coordination sphere formed by an N_2O_2 donor set of one L^2 ligand and one double-bond O atom, generating a 3D framework with the TEMPO radicals appended regularly in the pores (Figure 1b). **1** possesses open channels with dimensions of approximately 1.73 × 0.86 nm^2 along the *a* axis and a *PLATON*-calculated void space of ∼44.9%.[6] Topological analysis suggests that the framework of **1** can be described as a (3,3,3,4,4)-c net with the point symbol $(4.6.8)_2(4^2.6^4.8^5.10^4)(6^2.8)_2$ (Figure 1c).

Received: June 12, 2018

DOI: 10.1021/acs.inorgchem.8b01630
Inorg. Chem. XXXX, XXX, XXX−XXX

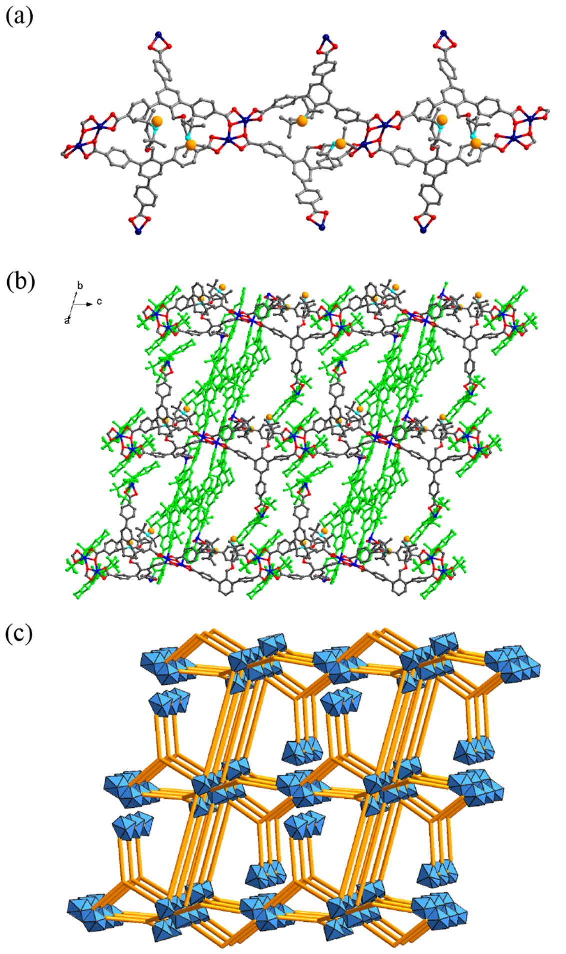

Figure 1. (a) View of the ribbonlike chain made up of $\mathbf{L}^1$ ligands and binuclear $\{Cd_2\}$ nodes. (b) 3D porous structure of **1**. Atoms: Cd, dark blue; O, red; N, turquiose; C, gray. The VO$\mathbf{L}^2$ ligands are drawn in bright green for clarity. The O atoms of TEMPO are shown as light-orange balls. (c) Topology of **1**.

TGA revealed that the framework is stable up to ~300 °C. The circular dichroism (CD) spectra of **1** made from (*R*)- and (*S*)-VO$\mathbf{L}^2$ are mirror images of each other in the solid state, suggesting their absolute configuration and enantiopurity. The porosity of **1** was evaluated by CO_2 sorption at 273 K. The typical type I isotherm indicated microporous materials, which gave an apparent Brunauer−Emmett−Teller (BET) surface area of 179 m^2/g. Dye-inclusion studies indicated ~1.5 methyl orange or 0.8 Rhodamine 6G dye uptake per formula unit for **1**, demonstrating retention of the porous framework structure in solution. A V $2p_{3/2}$ peak was observed at the binding energy of 516.4 eV in X-ray photoelectron spectroscopy (XPS) of **1**, confirming that V is in a +4 oxidation state.[7]

It has been established that TEMPO can promote the selective oxidation of alcohols[5d] and the VO(salen) complexes can efficiently catalyze the cyanosilylation of aldehydes.[8] Thus, the catalytic activity of **1** in sequential alcohol oxidation/asymmetric cyanation of aldehyde was assessed, and the transformation of *p*-bromobenzyl alcohol (**2a**) was selected as a model reaction. The oxidation process was carried out in a TEMPO/*tert*-butyl nitrite (TBN) system, which does not require any acid or base reagents. After optimization of the solvent, temperature, and molar ratio of the catalytic components, the oxidation reaction was conducted with 2 mol % **1** and 20 mol % TBN in 1, 2-dichloroethane under an O_2 atmosphere at 80 °C. The oxidation afforded 46%, 80%, and 92% conversions after 1, 4, and 7 h, respectively, and 99% conversion could be obtained if the reaction was continued for 8 h (Figure S11). TEMPO has been immobilized on a variety of solid supports to facilitate and further leverage its potential benefits, and this radical MOF represents one of the best solid catalysts for aerobic alcohol oxidation reported to date.[5d,9] Upon the completion of oxidation, the temperature was cooled to 0 °C, and trimethylsilyl cyanide (3.0 equiv) and triphenylphosphine oxide (1.0 equiv) were added to the reaction mixture under a N_2 atmosphere. The desired product **3a** was acquired in 98% conversion and 80% enantiomeric excess (ee) after 48 h.

Consequently, the scope and generality of the sequential process were studied. As shown in Table 1, benzyl alcohols with electron-withdrawing and -donating groups on the benzene ring were all well-tolerated, affording the corresponding products in excellent conversions (91−98%) with good enantioselectivities (75−87%; Table 1, entries 1−7). The positions of the substituents on the phenyl ring had a slight effect on the stereocontrol, and *p*-, *m*-, or *o*-methoxy (OMe)-substituted benzyl alcohols could give ~83%, 81%, and 87% ee, respectively. 1- and 2-naphthalenemethanol gave the desired products with 66% and 77% ee, respectively (Table 1, entries 8 and 9). When secondary alcohols were subjected to the reaction, only ketone products were obtained because **1** could not promote efficient cyanation of ketones (Table S5).

Table 1. Sequential Oxidation/Asymmetric Cyanation Reactions of Alcohols Catalyzed by 1[a]

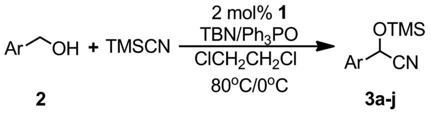

entry	Ar	3/conv (%)[b]	ee (%)[c]
1	*p*-Br	**a**/98 (78)	80 (65)
2	*p*-Cl	**b**/91	75
3	H	**c**/94 (85)	77 (72)
4	*p*-Me	**d**/93	77
5	*p*-OMe	**e**/96 (82)	83 (52)
6	*m*-OMe	**f**/91	81
7	*o*-OMe	**g**/94 (84)	87 (23)
8	1-naphthyl	**h**/75	66
9	2-naphthyl	**i**/78	77
10	*m*-G_0	**j**/<5 (45)	n.d. (n.d.)

[a] For reaction details, see the Supporting Information; the data in parentheses are results catalyzed by a mixture of $Me_3\mathbf{L}^1$ and VO$\mathbf{L}^2$ (the same amount of catalyst loadings as the MOF system). [b] Determined by ^1H NMR. [c] Determined by HPLC.

To examine whether the sequential reaction took place predominantly in the pores or on the surface of the framework, a bulky substrate bearing a G_0 group (ca. 2.0 × 1.9 × 1.4 nm^3) was synthesized and subjected to the reaction. MOF **1** gave an extremely low conversion (<5%) compared to its homogeneous analogue (45%), indicating that the bulky substrate could not access the catalytic sites because of its large diameter and catalysis does occur within the framework (Table 1, entry 10). The heterogeneous nature of the reaction was demonstrated by the fact that the supernatant from the sequential reaction after filtration did not afford any product.

DOI: 10.1021/acs.inorgchem.8b01630

The contribution of pore structures of the MOF catalyst was then evaluated by comparing the catalytic performance of **1** with that of the corresponding homogeneous system. A 1:2 mixture of Me_3**L**^{1} and VO**L**^{2} (the same catalyst loadings as the heterogeneous system) catalyzed the sequential reactions of *p*-bromobenzyl alcohol, benzyl alcohol, *p*-methoxybenzyl alcohol, and *o*-methoxybenzyl alcohol under identical conditions, affording the corresponding products **3a**, **3c**, **3e**, and **3g** in 78%, 85%, 82%, and 84% conversion with 65%, 72%, 52%, and 23% ee, respectively. Importantly, the difference in the catalytic performances became even more significant as the catalyst loading decreased (Table 2). At a loading of 1%, **1** and the Me_3**L**^{1}/VO**L**^{2} mixture afforded 72% and 51% conversion of **3a**, respectively. When the catalyst loading decreased to 0.5%, the conversion decreased to 42% for **1** and 19% for the homogeneous analogue. If the loading was further decreased to 0.2%, almost no product was detected for the homogeneous case, whereas **1** could still give 21% conversion. Structural investigation of **1** reveals that the TEMPO unit is in close contact with the VO(salen) site, with the shortest V—O(TEMPO) distance of ~10.8 Å, thus creating an attractive scaffold for synergistic catalysis. In the framework-confined system, the possibility for TEMPO and VO(salen) to meet each other increases, thereby leading to a dramatic catalytic difference with the homogeneous counterpart especially at a low catalyst concentration. In addition, the kinetic curves of the sequential reaction also revealed that integration of the TEMPO and VO(salen) species into one framework did enhance their catalytic activities and enantioselectivities (Figure S11). So, the framework displays an obvious confinement effect, and the chiral microenvironment, created by chiral metallosalen scaffolds, together with TEMPO, phenyl rings, and metal nodes, may be responsible for the improved catalytic performance.

Table 2. Sequential Oxidation/Asymmetric Cyanation Reactions of Alcohols Catalyzed by 1 and Related Homogeneous Catalysts at Different Catalyst Loadings[a]

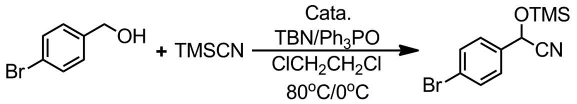

	1		homo[b]	
loading (mol %)	conv (%)	ee (%)	conv (%)	ee (%)
2	98	80	78	65
1	72	77	51	39
0.5	42	72	19	19
0.2	21	46	trace	n.d.

[a] For reaction details, see the Supporting Information; conversions were calculated by ^{1}H NMR; ee values were determined by HPLC. [b] Homo = a 1:2 mixture of Me_3**L**^{1} and VO**L**^{2} (the same catalyst loadings as the heterogeneous system).

The asymmetric cyanation reaction of aldehydes was also conducted with MOF **1**. Under similar conditions, *p*-bromobenzaldehyde, *p*-methoxybenzaldehyde, and *o*-methoxybenzaldehyde were successfully converted to the corresponding cyanohydrin silyl ethers in good conversion with 48%, 52%, and 63% ee, respectively. Obviously, **1**-catalyzed sequential oxidation/asymmetric cyanation reactions offer significantly higher (24−32%) ee values. The higher asymmetric induction was probably due to the formation of a tighter vanadium aldehyde transition state facilitated by the byproducts of TEMPO-catalyzed oxidation[10] and/or more distinct confinement effect of the framework catalyst in the sequential process.

After completion of the catalytic reaction, the framework catalyst can be recovered by simple filtration, which could be reused without the significant loss of activity and enantioselectivity. The conversions/ee values for the five consecutive runs are 94/87%, 92/85%, 91/85%, 91/84%, and 89/83%. PXRD showed that the recycled solid retained high crystallinity. The sample displayed a decreased BET surface area of 65 m^2/g, possibly because the partial framework collapsed. XPS showed that the recovered vanadium complex retained a +4 oxidation state.

In conclusion, we have demonstrated the successful synthesis of a chiral porous radical-decorated MOF. Integration of the TEMPO radicals and chiral VO(salen) active sites within a single framework endows the MOF as an effective heterogeneous catalyst for consecutive oxidation/asymmetric cyanation reactions with improved catalytic performance compared with its homogeneous counterpart. This work may extend the strategy to assemble multifunctional MOF catalysts, and taking advantage of this strategy, one can expect more heterogeneous catalysts with outstanding performance to be discovered.

ASSOCIATED CONTENT

Supporting Information

The Supporting Information is available free of charge on the ACS Publications website at DOI: 10.1021/acs.inorgchem.8b01630.

Experimental details and spectral data (PDF)

Accession Codes

CCDC 1588630 contains the supplementary crystallographic data for this paper. These data can be obtained free of charge via www.ccdc.cam.ac.uk/data_request/cif, or by emailing data_request@ccdc.cam.ac.uk, or by contacting The Cambridge Crystallographic Data Centre, 12 Union Road, Cambridge CB2 1EZ, UK; fax: +44 1223 336033.

AUTHOR INFORMATION

Corresponding Authors

*E-mail: liuy@sjtu.edu.cn.
*E-mail: yongcui@sjtu.edu.cn.

ORCID

Yan Liu: 0000-0002-7560-519X
Yong Cui: 0000-0003-1977-0470

Notes

The authors declare no competing financial interest.

ACKNOWLEDGMENTS

This work was supported by the National Natural Science Foundation of China (21522104, 21431004, and 21620102001), the National Key Basic Research Program of China (2016YFA0203400), the Key Project of Basic Research of Shanghai (17JC1403100 and 18JC1413200), and the Shanghai "Eastern Scholar" Program.

REFERENCES

(1) (a) Furukawa, H.; Cordova, K. E.; O'Keeffe, M.; Yaghi, O. M. The chemistry and applications of metal-organic frameworks. *Science* **2013**, *341*, 1230444. (b) O'Keeffe, M.; Yaghi, O. M. Deconstructing the Crystal Structures of Metal-Organic Frameworks and Related Materials into Their Underlying Nets. *Chem. Rev.* **2012**, *112*, 675−702. (c) Chughtai, A. H.; Ahmad, N.; Younus, H. A.; Laypkov, A.;

Verpoort, F. Metal-organic frameworks: versatile heterogeneous catalysts for efficient catalytic organic transformations. *Chem. Soc. Rev.* **2015**, *44*, 6804−6849. (d) Sumida, K.; Rogow, D. L.; Mason, J. A.; McDonald, T. M.; Bloch, E. D.; Herm, Z. R.; Bae, T.-H.; Long, J. R. Carbon Dioxide Capture in Metal-Organic Frameworks. *Chem. Rev.* **2012**, *112*, 724−781. (e) Li, J.-R.; Sculley, J.; Zhou, H.-C. Metal-Organic Frameworks for Separations. *Chem. Rev.* **2012**, *112*, 869−932. (f) Cui, Y.; Yue, Y.; Qian, G.; Chen, B. Luminescent Functional Metal-Organic Frameworks. *Chem. Rev.* **2012**, *112*, 1126−1162. (g) Cohen, S. M. Postsynthetic Methods for the Functionalization of Metal-Organic Frameworks. *Chem. Rev.* **2012**, *112*, 970−1000. (h) Kreno, L. E.; Leong, K.; Farha, O. K.; Allendorf, M.; Van Duyne, R. P.; Hupp, J. T. Metal-Organic Framework Materials as Chemical Sensors. *Chem. Rev.* **2012**, *112*, 1105−1125.

(2) (a) Huang, Y.; Liang, J.; Wang, X.; Cao, R. Multifunctional metal-organic framework catalysts: synergistic catalysis and tandem reactions. *Chem. Soc. Rev.* **2017**, *46*, 126−157. (b) Chen, Y.-Z.; Zhou, Y.-X.; Wang, H.; Lu, J.; Uchida, T.; Xu, Q.; Yu, S.-H.; Jiang, H.-L. Multifunctional PdAg@MIL-101 for One-Pot Cascade Reactions: Combination of Host−Guest Cooperation and Bimetallic Synergy in Catalysis. *ACS Catal.* **2015**, *5*, 2062−2069. (c) Yang, Q.; Xu, Q.; Jiang, H.-L. Metal−organic frameworks meet metal nanoparticles: synergistic effect for enhanced catalysis. *Chem. Soc. Rev.* **2017**, *46*, 4774−4808.

(3) (a) Song, F.; Zhang, T.; Wang, C.; Lin, W. Chiral porous metal-organic frameworks with dual active sites for sequential asymmetric catalysis. *Proc. R. Soc. London, Ser. A* **2012**, *468*, 2035−2052. (b) Song, F.; Wang, C.; Lin, W. A chiral metal-organic framework for sequential asymmetric catalysis. *Chem. Commun.* **2011**, *47*, 8256−8258. (c) Xia, Q.; Li, Z.; Tan, C.; Liu, Y.; Gong, W.; Cui, Y. Multivariate Metal-Organic Frameworks as Multifunctional Heterogeneous Asymmetric Catalysts for Sequential Reactions. *J. Am. Chem. Soc.* **2017**, *139*, 8259−8266. (d) Li, Z.; Liu, Y.; Xia, Q.; Cui, Y. Chiral binary metal-organic frameworks for asymmetric sequential reactions. *Chem. Commun.* **2017**, *53*, 12313−12316.

(4) (a) Fey, T.; Fischer, H.; Bachmann, S.; Albert, K.; Bolm, C. Silica-Supported TEMPO Catalysts: Synthesis and Application in the Anelli Oxidation of Alcohols. *J. Org. Chem.* **2001**, *66*, 8154−8159. (b) Karimi, B.; Farhangi, E. A Highly Recyclable Magnetic Core-Shell Nanoparticle-Supported TEMPO Catalyst for Efficient Metaland Halogen-Free Aerobic Oxidation of Alcohols in Water. *Chem. - Eur. J.* **2011**, *17*, 6056−6060. (c) Ferreira, P.; Hayes, W.; Phillips, E.; Rippon, D.; Tsang, S. C. Polymer-supported Nitroxyl Catalysts for Selective Oxidation of Alcohols. *Green Chem.* **2004**, *6*, 310−312. (d) Xu, F.; Xu, H.; Chen, X.; Wu, D.; Wu, Y.; Liu, H.; Gu, C.; Fu, R.; Jiang, D. Radical Covalent Organic Frameworks: A General Strategy to Immobilize Open-Accessible Polyradicals for High-Performance Capacitive Energy Storage. *Angew. Chem., Int. Ed.* **2015**, *54*, 6814−6818. (e) Hughes, B. K.; Braunecker, W. A.; Bobela, D. C.; Nanayakkara, S. U.; Reid, O. G.; Johnson, J. C. Covalently Bound Nitroxyl Radicals in an Organic Framework. *J. Phys. Chem. Lett.* **2016**, *7*, 3660−3665. (f) Brunel, D.; Fajula, F.; Nagy, J. B.; Deroide, B.; Verhoef, M. J.; Veum, L.; Peters, J. A.; van Bekkum, H. Comparison of Two MCM-41 Grafted TEMPO Catalysts in Selective Alcohol Oxidation. *Appl. Catal., A* **2001**, *213*, 73−82.

(5) (a) Maspoch, D.; Ruiz-Molina, D.; Wurst, K.; Domingo, N.; Cavallini, M.; Biscarini, F.; Tejada, J.; Rovira, C.; Veciana, J. A nanoporous molecular magnet with reversible solvent-induced mechanical and magnetic properties. *Nat. Mater.* **2003**, *2*, 190−195. (b) Faust, T. B.; D'Alessandro, D. M. Radicals in Metal-Organic Frameworks. *RSC Adv.* **2014**, *4*, 17498−17512. (c) Li, L.; Matsuda, R.; Tanaka, I.; Sato, H.; Kanoo, P.; Jeon, H. J.; Foo, M. L.; Wakamiya, A.; Murata, Y.; Kitagawa, S. A Crystalline Porous Coordination Polymer Decorated with Nitroxyl Radicals Catalyzes Aerobic Oxidation of Alcohols. *J. Am. Chem. Soc.* **2014**, *136*, 7543−7546. (d) Zwoliński, K. M.; Chmielewski, M. J. TEMPO-Appended Metal-Organic Frameworks as Highly Active, Selective, and Reusable Catalysts for Mild Aerobic Oxidation of Alcohols. *ACS Appl. Mater. Interfaces* **2017**, *9*, 33956−33967.

(6) Spek, A. L. Single-crystal structure validation with the program PLATON. *J. Appl. Crystallogr.* **2003**, *36*, 7−13.

(7) Yano, H.; Ono, C.; Shiroishi, H.; Saito, M.; Uchimoto, Y.; Okada, T. High CO Tolerance of N,N-Ethylenebis(salicylideneaminato)-oxovanadium(IV) as a Cocatalyst to Pt for Anode of Reformate Fuel Cells. *Chem. Mater.* **2006**, *18*, 4505−4512.

(8) Xi, W.; Liu, Y.; Xia, Q.; Li, Z.; Cui, Y. Direct and Post-Synthesis Incorporation of Chiral Metallosalen Catalysts into Metal-Organic Frameworks for Asymmetric Organic Transformations. *Chem. - Eur. J.* **2015**, *21*, 12581−12585.

(9) (a) Huangfu, Y.; Sun, Q.; Pan, S.; Meng, X.; Xiao, F. Porous Polymerized Organocatalysts Rationally Synthesized from the Corresponding Vinyl-Functionalized Monomers as Efficient Heterogeneous Catalysts. *ACS Catal.* **2015**, *5*, 1556−1559. (b) Karimi, B.; Vahdati, S.; Vali, H. Synergistic catalysis within TEMPO-functionalized periodic mesoporous organosilica with bridge imidazolium groups in the aerobic oxidation of alcohols. *RSC Adv.* **2016**, *6*, 63717−63723. (c) Karimi, B.; Mirzaei, H. M.; Farhangi, E. Fe_3O_4@SiO_2-TEMPO as a Magnetically Recyclable Catalyst for Highly Selective Aerobic Oxidation of 5-Hydroxymethylfurfural into 2,5-Diformylfuran under Metal- and Halogen-Free Conditions. *ChemCatChem* **2014**, *6*, 758−762.

(10) Belokon, Y. N.; Clegg, W.; Harrington, R. W.; Maleev, V. I.; North, M.; Pujol, M. O.; Usanov, D. L.; Young, C. Mechanism-Guided Development of VO(salen)X Complexes as Catalysts for the Asymmetric Synthesis of Cyanohydrin Trimethylsilyl Ethers. *Chem. - Eur. J.* **2009**, *15*, 2148−2165.